Quaternary Science Reviews 259 (2021) 106900

Contents lists available at ScienceDirect

Quaternary Science Reviews

journal homepage: www.elsevier.com/locate/quascirev

Patterns of alluvial deposition in Andean lake consistent with ENSO trigger

Kimberley Hagemans [a, *], Kees Nooren [a], Tjalling de Haas [a], Mario Córdova [b], Rick Hennekam [c], Martin C.A. Stekelenburg [a], Donald T. Rodbell [d], Hans Middelkoop [a], Timme H. Donders [a]

[a] Department of Physical Geography, Faculty of Geosciences, Utrecht University, Princetonlaan 8a, 3584 CB, Utrecht, the Netherlands
[b] Departamento de Recursos Hídricos y Ciencias Ambientales, Universidad de Cuenca, Cuenca, Ecuador
[c] Department of Ocean Systems, NIOZ Royal Netherlands Institute for Sea Research, the Netherlands
[d] Geology Department, Union College, Schenectady, NY, USA

ARTICLE INFO

Article history:
Received 24 September 2020
Received in revised form
23 December 2020
Accepted 8 March 2021
Available online 31 March 2021

Handling Editor: Yan Zhao

Keywords:
Laguna Pallcacocha
Flood layer
El Niño
Debris flow
Andean meteorology

ABSTRACT

The laminated sediment record from Laguna Pallcacocha, Ecuador, is widely used as a sensitive recorder of past variability in the El Niño-Southern Oscillation. However, limited knowledge of local meteorology, hydrogeomorphic processes, and the lateral variability of the lacustrine stratigraphy have resulted in some ambiguity in proxy interpretation. In this study, we report new high-resolution meteorological data, hydrogeomorphic mapping of the catchment and geochemistry of the lake's sediments. We show that the fine clastic layers are deposited from alluvial activity in the catchment related to intensive rainfall events originating from the Pacific. Frequency analyses of the geochemistry of the sediments indicates that the clastic layers in L. Pallcacocha fall into the characteristic ENSO frequency band and most likely record Eastern Pacific and Coastal Pacific El Niño events. We also illustrate that recent debris flow deposition has resulted in an abrupt avulsion of the main fluvial channels, redirecting sediment input between the lake's two basins and possibly influencing the lithostratigraphy of the sediment package of L. Pallcacocha.

1. Introduction

Laminated sediment deposits are sensitive recorders of paleoclimatic change and are frequently interpreted in terms of flood and run-off variations (Bussmann and Anselmetti, 2010; Moy et al., 2002; Rubensdotter and Rosqvist, 2009). The tropical Andean lake Laguna Pallcacocha (SW Ecuador) is a well-known example, of which clastic laminae frequencies are considered to represent the Holocene evolution of the El Niño Southern Oscillation (ENSO) (Moy et al., 2002; Rodbell et al., 1999). Implicit to the reconstruction of paleoclimate from this and other laminated records is the identification of catchment characteristics and runoff processes that affect the ability of lacustrine sedimentary proxies to record climatic change (Corbett and Munroe, 2010). The detrital flood layer record of lakes has been linked to mass movements occurring in their upper catchment (Rubensdotter and Rosqvist, 2009). Although heavy rainfall events have been identified as the main cause of debris flow and sediment runoff from hillslopes into streams and lakes (Colombaroli et al., 2018; Glur et al., 2013; Lamoureux, 2002; Swierczynski et al., 2013), the unambiguous registration of these events in lake sediments remains notoriously difficult (Rubensdotter and Rosqvist, 2009). This is because the sediment transport system (sediment cascade) is often complex with temporary storage of sediment along this cascade by redeposition in riparian settings, which can be a major factor influencing the flood signal recorded in down valley lakes (Rubensdotter and Rosqvist, 2009).

Inferring past ENSO variability from laminated sediments without considering hydrogeomorphological mechanisms behind such flood layer records can result in inconsistent or biased paleoclimate reconstructions. Such reconstructions should preferably be based on multiple cores within a depositional basin to separate lateral shifts of feeding channels within the depositional basin from climate signals. In the case of L. Pallcacocha, the original

* Corresponding author.
E-mail address: Kim.Hagemans.science@gmail.com (K. Hagemans).

https://doi.org/10.1016/j.quascirev.2021.106900

interpretation of the flood layer record was based on the concept that Pacific convective precipitation during warm ENSO events erodes the volcanic bedrock in the catchment and initiates debris-flow activity in the drainage basin of the lake (Rodbell et al., 1999; Moy et al., 2002). Periods of increased stream discharge during intense rainfall events and associated enhanced sediment delivery by the stream that enters the lake have resulted in the deposition of a laminated sediment record that, reportedly, documents the evolution of ENSO through the Holocene (Moy et al., 2002; Rodbell et al., 1999). However, independent analyses of new sediment cores from L. Pallcacocha in the context of local meteorological records have led to the suggestion that the laminated sediments of L. Pallcacocha may not be a conclusive recorder of paleo-ENSO activity (Schneider et al., 2018). Yet, these analyses did not consider the hydrogeomorphology of the catchment. Furthermore, the meteorological data used in the analyses only covered precipitation totals at daily and 72-h time intervals (Schneider et al., 2018), which is too coarse to identify intense rainfall events that are typically characterized by their short duration of a few hours only in the tropical Andes (Padrón et al., 2015). Furthermore, the presence of two sub basins is a hydrogeomorphological characteristic of L. Pallcacocha (Schneider et al., 2018), but data on in-lake lateral variability of top sediments, important for signal calibration, was not included in previous analyses. Hence, the exact relation between meteorological processes, hydrogeomorphic properties of the catchment and in-lake sediment accumulation patterns have led to ambiguity in the interpretation of the flood layer record of L. Pallcacocha as a recorder of paleo-ENSO variability.

Here, we study local variations in the hydrogeomorphology, lateral variability and lithostratigraphy of the flood layer record from L. Pallcacocha. Our objective is to improve the understanding of Pallcacocha's sedimentary proxies and to test its ability to record past ENSO variability. We use new 5-min resolution meteorological data from a local station to identify short rainfall events of sufficient intensity to generate debris flows in the L. Pallcacocha catchment. We map the hydrogeomorphic processes that occurred over the same period in the catchment and document the lateral variability of flood deposits recorded in L. Pallcacocha and deltaic sediments. We use detailed ^{210}Pb geochronology to date recent sediment accumulation of the two sub basins of L. Pallcacocha and test the consistency of the flood deposition signal with multiple core scanning technologies.

2. Methods and materials

2.1. Study region and study site

L. Pallcacocha (4050 masl) is located in the Cajas National Park (CNP), ca. 25 km of Cuenca, in the western Cordillera of the southern Ecuadorian Andes (2°46′46″S, 79°13′27″W) (Fig. 1). The lake has a small catchment of 1.5 km^2 and a lake surface area of 0.05 km^2. Depth soundings were carried out in 2015 to establish the bathymetry of the lake. Input into the lake come from catchment

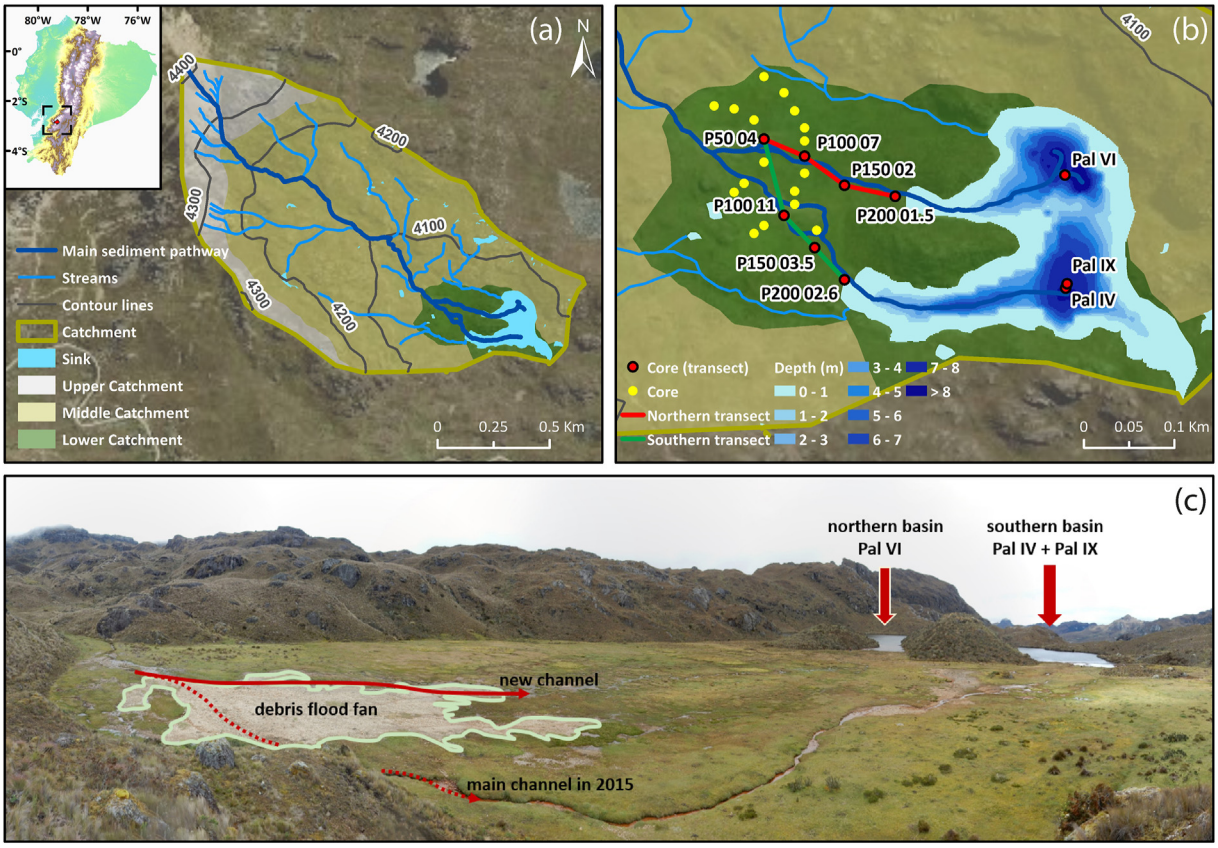

Fig. 1. Study area, geomorphological setting and coring locations. a) L. Pallcacocha is situated on the western Andean Cordillera of Ecuador. The upper catchment is characterized by steep slopes and exposed bedrock. In the middle catchment, temporary storage of sediment occurs along the main transport pathways. The lower catchment is mostly covered by the alluvial fan. b). Yellow dots show coring locations across the alluvial fan, red dots show coring transect A-A' (northern transect) and B–B' (southern transect). The bathymetric map shows the presence of two sub basins in the lake and lake coring locations. c) Photograph of the middle and lower catchment of L. Pallcacocha, showing the most recent debris flood fan, the fluvial channels on the alluvial fan and the two basins of the lake. (For interpretation of the references to colour in this figure legend, the reader is referred to the Web version of this article.)

runoff, direct precipitation, and output occurs via river outflow and evaporation. Retention time of the lake is about 0.5 yr. The vegetation in the catchment is dominated by páramo tussock grass, while the alluvial fan is dominated by marsh and semi-aquatic vegetation (Hagemans et al., 2019). The park has been protected since 1977 under Ecuador's National System of Protected Areas and was declared a UNESCO biosphere reserve in 2013 (Ministerio del Ambiente del Ecuador, 2018). The bedrock in the L. Pallcacocha catchment is dominated by rocks from the volcanoclastic Tarqui formation that show few traces of weathering. Total watershed length is 1.8 km with an average channel slope of 16%. Three main geomorphological units can be distinguished in the L. Pallcacocha catchment (Fig. 1). The upper catchment (4250–4413 m asl) is characterized by steep slopes and exposed bedrock at two sites covering ~9% of the 98 ha catchment of the main sediment pathway above the apex of the alluvial fan (Fig. 1). On the steep slopes numerous traces of debris flow activities occur. In the middle catchment (4050–4250 m asl) temporary storage of sediment occurs along the main transport pathways. The lower catchment (4050 m asl) is partly covered by a relatively large alluvial fan.

2.2. Hydrogeomorphology and meteorology

The potential for debris flow initiation in the L. Pallcacocha catchment was determined by 1) the geomorphometry and geomorphology of the catchment (Bertrand et al., 2013; Wilford et al., 2004), 2) the availability of abundant erodible sediment (Bovis and Jakob, 1999), and 3) the occurrence of intense rainfall events that exceed the rainfall intensity-duration threshold for debris flow generation (Guzzetti et al., 2008). To document the location and occurrence of recent debris flow events, the hydrogeomorphology and land cover of the L. Pallcacocha catchment area were investigated through satellite imagery interpretation, vegetation surveys and field observations in 2015 and 2018 (Hagemans et al., 2019). We conducted spatial analyses with ArcGIS software (version 10.3.1, ESRI, Redlands, CA, US) to determine hillslope angles and to identify sediment pathways, buffer zones and sediment connectivity between the slope and the channel system following (Fryirs et al., 2007; Heckmann et al., 2018). To assess whether the geometry of L. Pallcacocha allows for the generation of debris flows, we compared its geometry to geomorphic relations combining Melton ratio (relief divided by the square root of catchment area) with watershed length (Wilford et al., 2004) and with channel slope (Bertrand et al., 2013), which are commonly used metrics to determine whether debris flows or water floods dominantly form in a catchment.

Rainfall events exceeding the rainfall intensity-duration threshold required for debris flow initiation were identified by analysing 5-min precipitation totals for the period February 2013 and December 2017 from the nearby weather station Toreadora, situated ca. 1.7 km southeast of L. Pallcacocha. The weather station was installed at the end of 2012 by the University of Cuenca (Carrillo-Rojas et al., 2016). Wind speed and direction measurements from the weather station were used to determine origin of rainfall events. The most intensive rainfall events with 5-min precipitation totals $\geq$1.5 mm (18 mm/h) were selected and tested on their potential to generate debris flow events, based on available empirical thresholds for debris flow generation in mountainous areas worldwide (Guzzetti et al., 2008). ENSO data was retrieved from NOAA (2020).

2.3. Sediment sampling, chronology and XRF

In August 2015 and July 2018 three sediment cores from the southern (cores Pal IV and Pal IX, both ~45 cm) and northern (core Pal VI, ~85 cm) sub basin of L. Pallcacocha were collected with an UWITECH gravity corer. Additionally, a sediment core reaching to a depth of 6 m was obtained from the deepest part of the northern lake basin with a square-rod piston corer (Pal VII and Pal VIII), which however did not yield a continuous record due to coring problems.

Light coloured clastic layers in the lake sediments were identified through visual inspection, computer tomography (CT) core photography, and X-ray fluorescence (XRF) core scanning. XRF core scanning on Pal IV, Pal VI and Pal IX was conducted with an Avaatech scanner at the Royal Netherlands Institute for Sea Research (NIOZ). All cores were scanned at 10 kV and 30 kV at 1 mm resolution. We focus on the Br/Ti log-ratio, as log-ratios provide straightforward interpretable signals of variability in chemical composition (Weltje and Tjallingii, 2008), and the ratio of incoherent (Compton) to coherent (Rayleigh) X-Ray scattering peaks (i.e., incoh/coh). Computer tomography (CT) scans were conducted with a Siemens Somaton Definition Flash at the Meander Medical Centre in Amersfoort, the Netherlands. Pal IX and Pal IV were scanned with dual energy at 100 kV and 140 kV. An additional X-ray scan was made on the Pal IV sediment core at 50 kV with a Faxitron X-Ray System at the NIOZ. The line-scan camera in the Avaatech scanner at NIOZ was used to produce images of all core material, yielding high-resolution (71.4 μm pixel resolution) images including colour intensity data.

The age-depth models of the sediment cores from L. Pallcacocha are based on ^{210}Pb, and ^{226}Ra isotopes analysed at Utrecht University in 0.5 cm intervals. A chronology for both cores was established using a constant-rate-of-supply (CRS) model (Sanchez-Cabeza and Ruiz-Fernández, 2012) (Fig. 2) We applied the age-depth model for fluvio-lacustrine deposits by Minderhoud et al. (2016) to account for fluctuations in sedimentation rates in both records. The high resolution ^{210}Pb dating and measurements of red colour intensity (high RCI is high sedimentation rate; Moy et al., 2002) provided a tool to express the variation between clastic sediment input from the Pallcacocha catchment and the autochthonous organic deposition in the lake itself. Since the northern basin was cored for the first time, % total organic carbon (TOC) was determined for PAL VI by loss on ignition (LOI) at 550 °C of oven-dried sediment aliquots, following Heiri et al. (2001). For core Pal IV, RCI, Br/Ti, and incoh/coh ratios were analysed for periodicities with spectral time series analyses using RED FIT (Schulz and Mudelsee, 2002) implemented in PAST version 3.25 (Hammer et al., 2001). RED FIT analyses irregularly-spaced time series and determines significance relative to an autoregressive red noise model (we used the following settings for the analyses: window: rectangle, oversample: 2 and segments: 2). Also, in 2018, sediment cores were collected along several coring transects in the L. Pallcacocha catchment with the objective to map the surface variability and Holocene infill of the alluvial fan. Sedimentological descriptions of these cores were made at 10 cm intervals and followed USDA soil classifications (Fig. 3).

3. Results

3.1. Core descriptions

Sediment cores Pal IV and IX from the central part of the southern basin reproduce the sediment sequence reported by Rodbell et al. (1999) (Fig. 4). The cores consist of dark organic-rich gyttja with frequent light-coloured inorganic laminae (Rodbell et al., 1999). The laminations are sharply delineated, do not show signs of bioturbation and the reported total organic carbon (TOC)

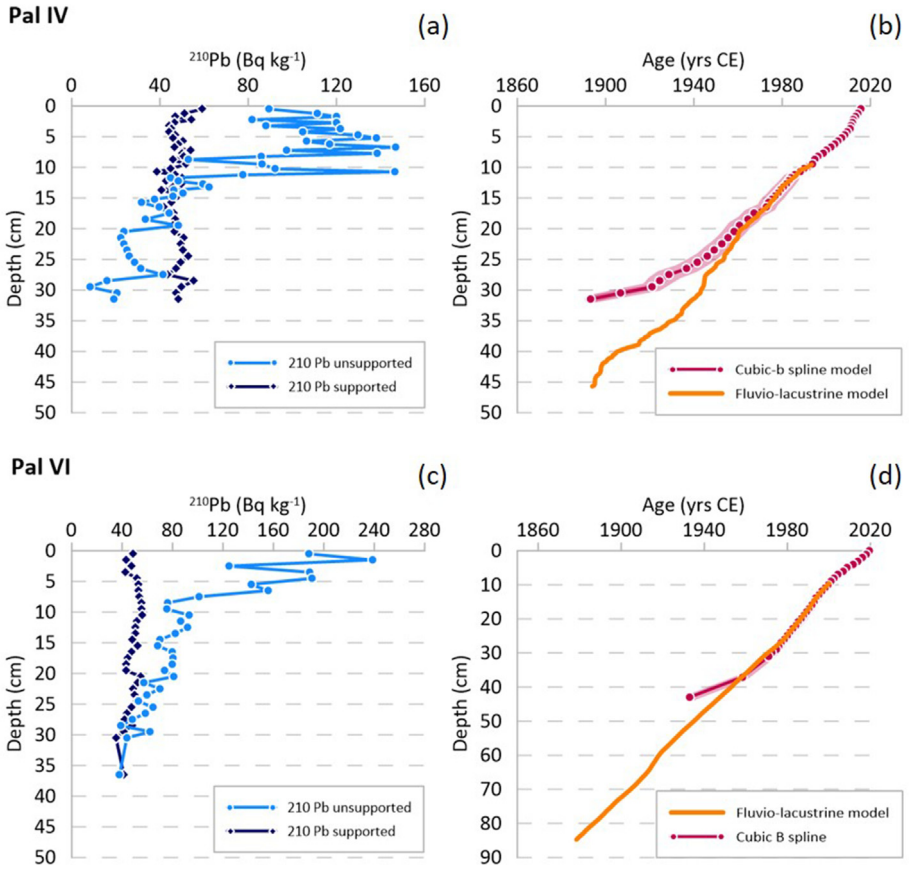

Fig. 2. Age models for cores Pal IV and Pal VI. a) ^{210}Pb activities throughout core Pal IV from the Southern basin of Laguna Pallcacocha. b). Constructed age model for Laguna Pallcacocha showing the fluvio-lacustrine model and the Cubic-b spline model. c) ^{210}Pb activities throughout core Pal IV from the Northern basin of Laguna Pallcacocha. d) Constructed Cubic-B spline age model for Laguna Pallcacocha.

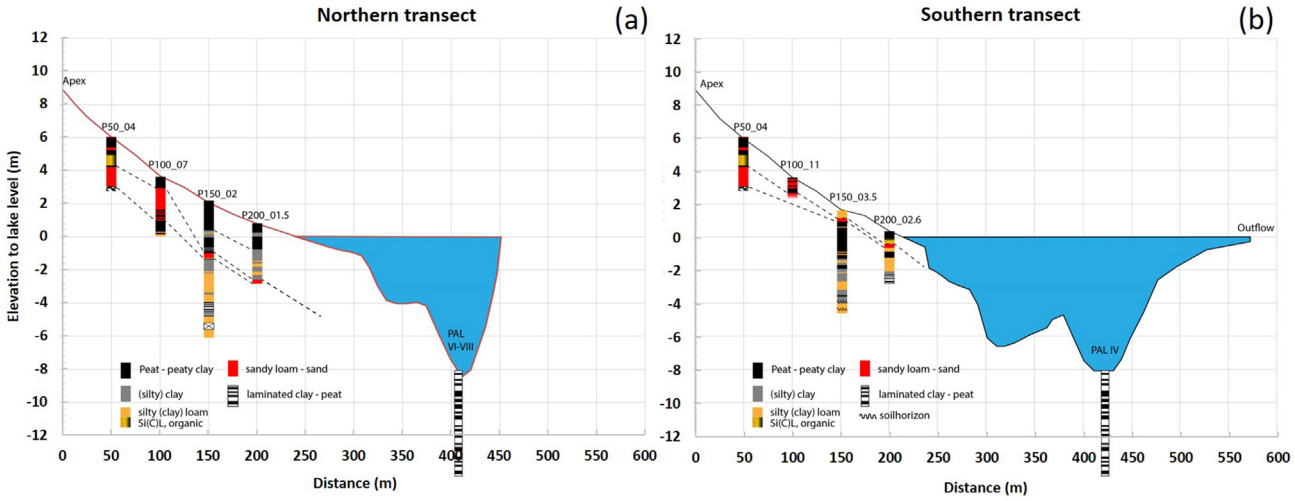

Fig. 3. Cross sections of the sedimentological mapping of the alluvial fan of Laguna Pallcacocha. The two transects show the spatial variability of the subsurface of the alluvial fan. The cross sections reveal the presence of laminated clay-peat sediments below the alluvial fan deposits, indicating that presence of several sub basins the past that have been partially filled in through time.

within the clastic laminae is ~2%, while the dark organic-rich intervals contain >10% organic C. The top 9 cm is distinctly different from the rest of the core and has a high clastic content throughout, but does not show signs of disturbance. The clastic laminae are light yellow in colour and vary in thickness between ~2 and 15 mm.

Core Pal VI from the northern basin shows a much less distinct lamination pattern in comparison to Pal IV and Pal IX (Fig. 4). Laminae are less frequent and only defined in the RCI data at 9–10 cm and 62–64 cm depth. In the field, a weakly defined lamination was visible immediately after coring, however, exposure

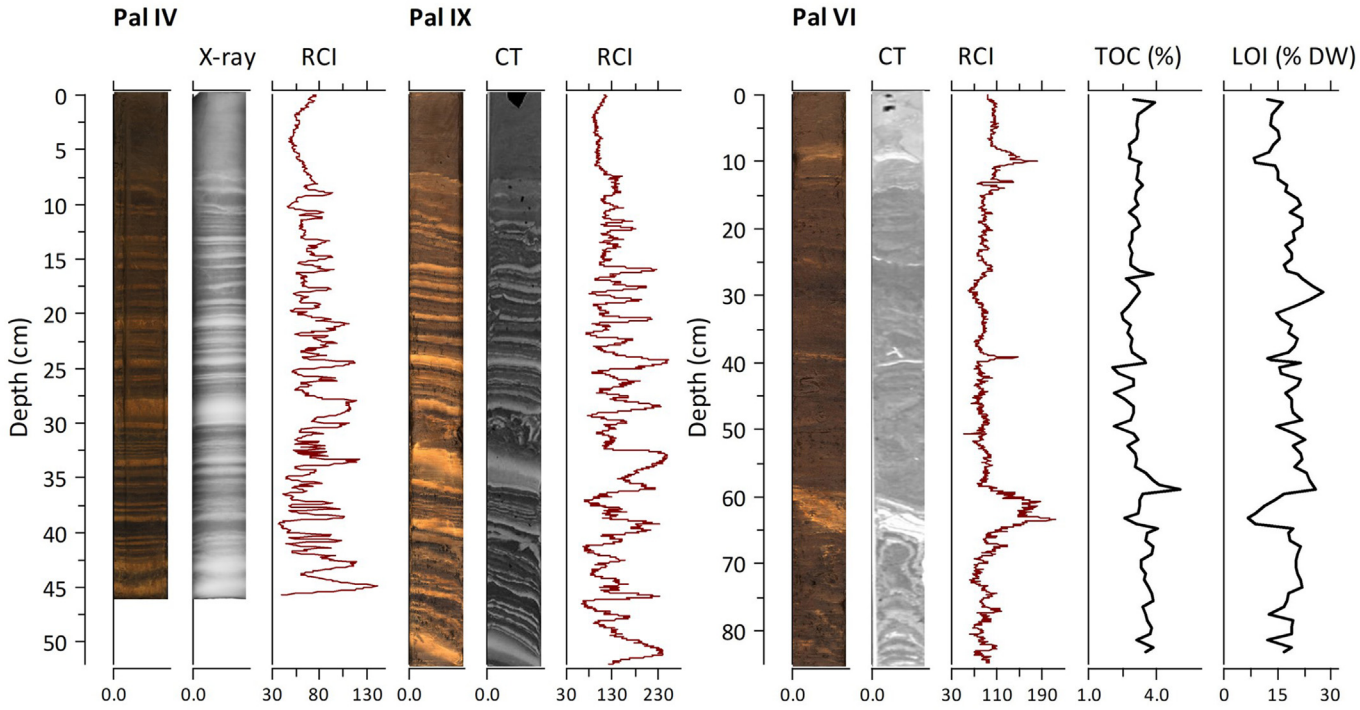

Fig. 4. Lithostratigraphy, X-ray and CT scan images and red color intensity for cores Pal IV and Pal IX collected from the southern basin and core Pal VI collected from the northern basin. Since the northern basin was cored for the first time % total organic carbon (TOC) was determined for PAL VI by loss on ignition (LOI). (For interpretation of the references to colour in this figure legend, the reader is referred to the Web version of this article.)

to oxygen caused loss of this pattern. The majority of the core is dark grey in colour and LOI analysis shows a TOC of around 20% (Fig. 4). The few well defined laminae contain around 10% TOC and have a distinctly lower water content. These relatively high TOC values, relative to the southern basin, reflect overall low sediment input to the northern basin. The clastic component is fine-grained, clay-to silt-sized throughout. The clastic laminae, while lower in TOC, show no visible change in grain size.

3.2. The sediment cascade and meteorology

The upper catchment (4250–4413 m asl), which is split into two sub-catchments, has a Melton ratio, watershed length, and channel slope consistent with debris flow generation (Fig. 5). This means that debris flows are likely triggered when rainfall exceeds the local rainfall intensity-duration threshold for debris-flow formation (Fig. 5). During the fieldwork in July 2018 we observed a new debris flow deposit near the apex of the alluvial fan (Fig. 1) that was most likely formed in 2016, as inferred from satellite imagery. This deposit choked the former main channel that drained towards the southern basin of lake Pallcacocha, thus redirecting river discharge through several new channels that drain towards Pallcacocha's northern basin. In July 2018 we observed that the principal discharge continued to be routed to these northern channels

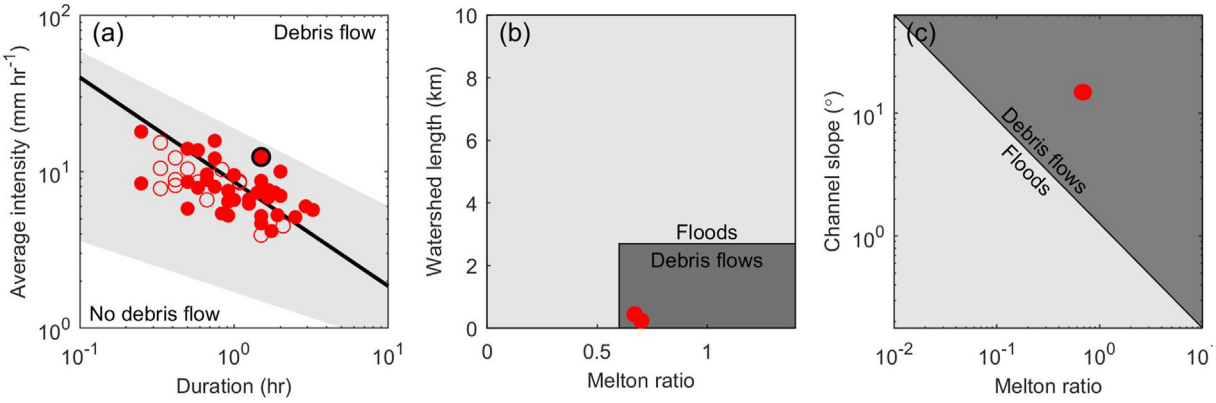

Fig. 5. Debris flow thresholds and Melton ratios. a) Rainfall intensity-duration thresholds for debris-flow generation (after Guzzetti et al., 2008). The gray band indicates the extent of all thresholds worldwide, while the black line indicates the threshold for mountainous areas which is most relevant for L. Pallcacocha. The data points show the 49 most heavy rainfall events in the period February 2013 and December 2017. Closed circles are events from the west and open circles are events from the east. The black outline shows the 2016 event that led to debris flow deposition on the fan (Fig. 1). b-c) Melton ratio versus watershed length (after Wilford et al., 2004) and channel slope (after Bertrand et al., 2013), indicating debris flow and flood regimes. The red dots show the values of the two sub-catchments of L. Pallcacocha, indicating that debris flows are most likely generated. (For interpretation of the references to colour in this figure legend, the reader is referred to the Web version of this article.)

(Fig. 1C). The alluvial fan contains a dense network of small channels, avulsion features, and shows evidence of reworking of older alluvial deposits. Overall, we distinguish a main sediment pathway from the largest bedrock exposure on the steep slopes, across the alluvial fan towards the lake. Bathymetry of the lake shows the occurrence of two sub basins, each with a maximum depth of approximately 8 m separated by a sill of circa 2 m depth (Fig. 1).

In the meteorological data, we identified 49 intense rainfall events (Fig. 6) which we separated into two clusters: 1) those that are associated with a dominant WSW wind, and 2) those associated variable wind patterns. All events in cluster 1 reach an intensity of 30 mm h^{-1}, during which wind direction is predominantly WSW, in contrast to mostly easterly winds during non-rain event windows. Events in cluster 2 are marked by lower rainfall intensities, more variable wind patterns and less well-defined rainfall events. The highest intensity event recorded on October 1st, 2016 was most likely the event that triggered the recent debris flow deposit on the alluvial fan (Figs. 5 and 6). Eastern wind dominated during the week preceding the event, while the dominant wind direction during the interval of intense rainfall was from the Pacific (WSW).

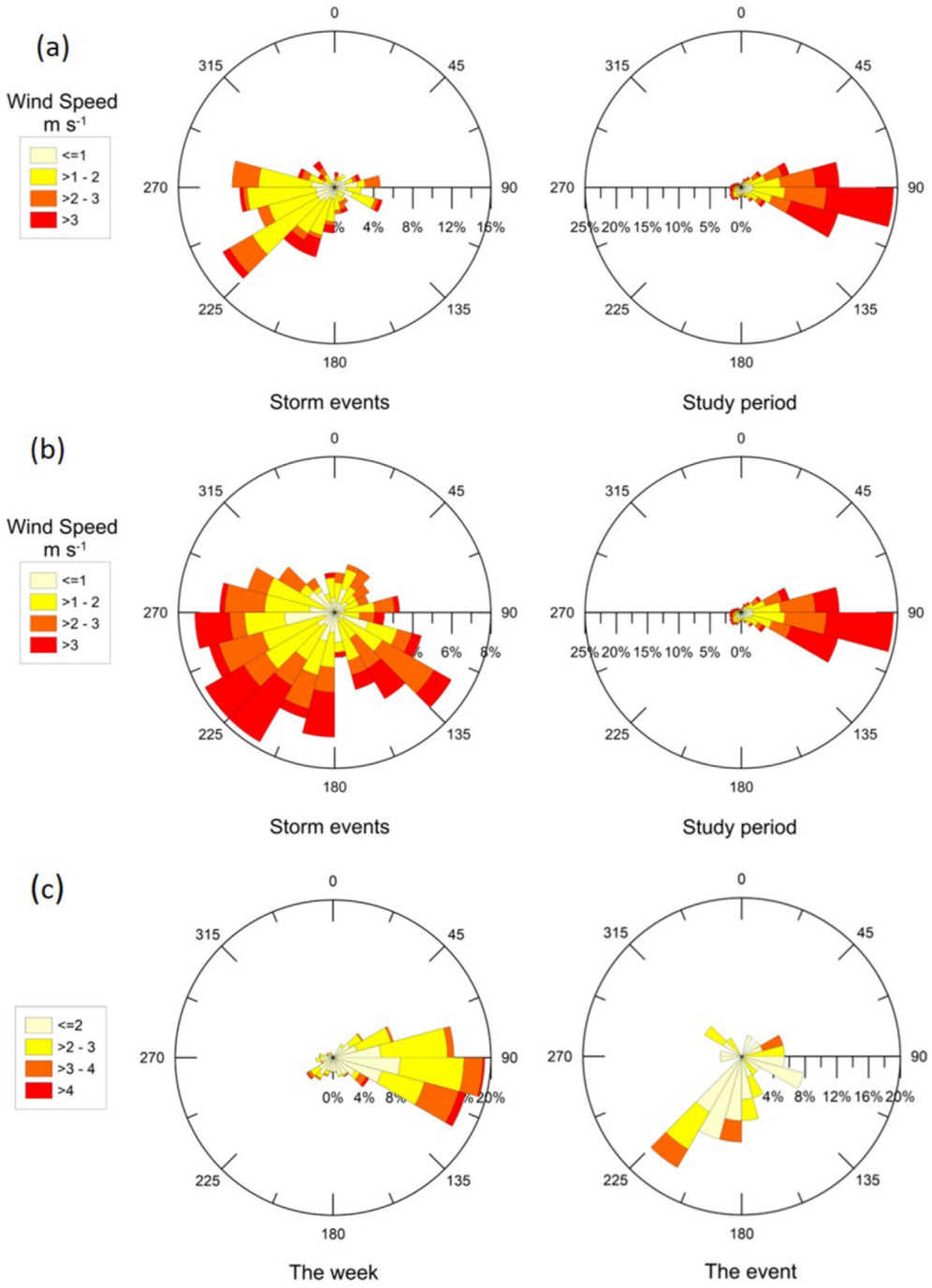

Fig. 6. Meteorology. a) Intense rainfall events in cluster 1: Wind direction during the identified high-intensity rainfall events is predominantly from WSW. Wind direction during the total study period is from the Amazon. b) Intense rainfall events in cluster 2: Wind direction is more variable compared to cluster 1. c) The intense rainfall event on October 1st 2016 that most likely triggered the recent debris flow resulting in the deposit on the alluvial fan.

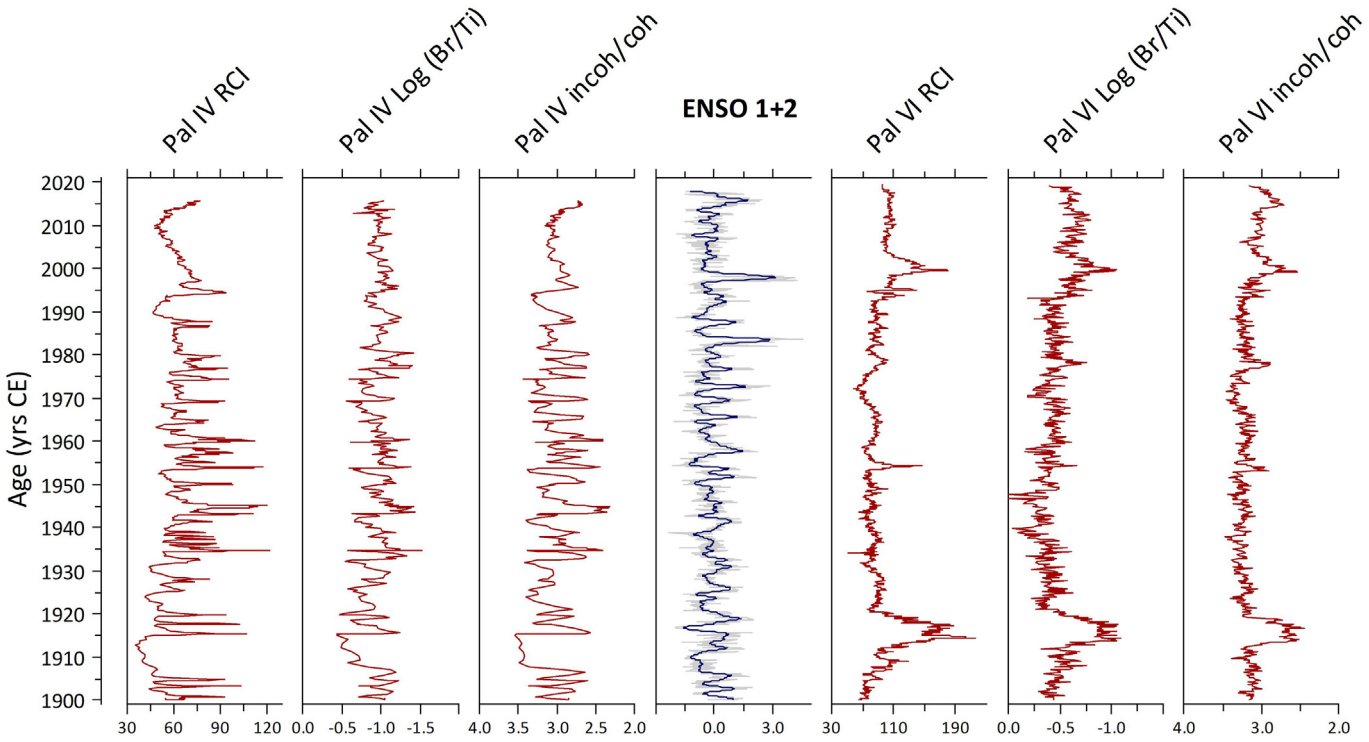

Fig. 7. Geochemistry of the lake sediments. X-ray image of Pal IV and CT images of Pal IX and Pal VI, red color intensity (RCI) and log (Br/Ti) ratios for Pal IV and Pal VI. El Niño 1+2 index shows the occurrence of El Niño events in the eastern Pacific. Peaks in the RCI, Log (Br/Ti) and incoh/coh ratios correspond with clastic laminae in the sediment core (see Fig. 4). (For interpretation of the references to colour in this figure legend, the reader is referred to the Web version of this article.)

3.3. The flood layer record

Sedimentological mapping of the alluvial fan showed the presence of lacustrine deposits below the alluvial fan deposits (Fig. 3), indicating that the basins have been partially filled in, and that several sub basins were present in the past. Coarse alluvial fan deposits close to the southern basin blocked deep coring which precluded the mapping of the total extent of infilled alluvial fan basins. Cores Pal IV and Pal IX from the southern basin of L. Pallcacocha both show light-coloured fine clastic laminae interbedded with dark-coloured organic rich laminae (Fig. 4). The laminated section of the cores can be directly correlated to other cores collected by previous research expeditions to the southern basin of L. Pallcacocha (Moy et al., 2002; Schneider et al., 2018). This indicates a strong consistency of lake infill laminations across the southern basin. The ^{210}Pb age control points indicate that the most recent clear sediment layer at ~9.5 cm sediment depth in the southern basin was deposited around 1993. The RCI, Br/Ti and incoh/coh records from Pal IV reveal a close match between the timing of clastic laminae and the ENSO 1+2 index maxima (Fig. 7). Out of the 21 moderate to very strong El Niño events that occurred between 1900 and 2015 CE, 20 events correlate within 1 or 2 years to pronounced clastic laminae in the composite record. The time series analyses (RED FIT) shows significant 3, 5 and 7-year frequencies for RCI and Br/Ti and incoh/coh ratios in the sediment core Pal IV (Fig. 8).

4. Discussion

4.1. Potential for debris flow generation and the sediment cascade

Recorded local rainfall events are strong enough to initiate debris flows in the catchment of L. Pallcacocha and can generate clastic layers in the lake, although our high-resolution meteorological record is too short to record multiple ENSO events. These local rainfall events originate from the Pacific, based on the correspondence of westerly winds during intervals of most intense precipitation. Mesoscale weather prediction models have indeed shown that the Pallcacocha region receives extreme precipitation through convective bursts originating from the Pacific. This particularly occurs during coastal El Niño and Eastern Pacific ENSO events (Kiefer and Karamperidou, 2019). The number of such modeled threshold-exceeding precipitation events in the high Andes correspond to the number of events identified in the original late Holocene L. Pallcacocha record (Kiefer and Karamperidou, 2019).

Intense Pacific-derived rainfall events mobilize the easily weatherable volcaniclastic sediment on the steep slopes of the upper catchment and produce substantial amounts of loose sediment to the fluvial channels in the catchment. Given the relatively large unstable zone of exposed bedrock and the high density network of shallow channels, we infer that the catchment is transport-limited, where enough sediment is available to form debris flows. In such basins, debris flow frequency is controlled primarily by the frequency of extreme hydroclimatic events, in contrast to basins were the supply of mobilizable sediment is a limiting condition (e.g. Bovis and Jakob, 1999). The finer-grained clastic sediments of the debris flow deposits in the catchment are easily entrained and transported through the channels to the lake by subsequent smaller floods. Indeed, in the middle catchment, the main traces of sediment erosion and transportation processes show active erosion of stream beds and banks made of previously deposited sediments. The reworking of stored sediment is the primary source of the fine-grained sediments deposited in the lake during intense rainfall events. Deposition of debris flows and alluvial sediments has resulted in expansion and progradation of the

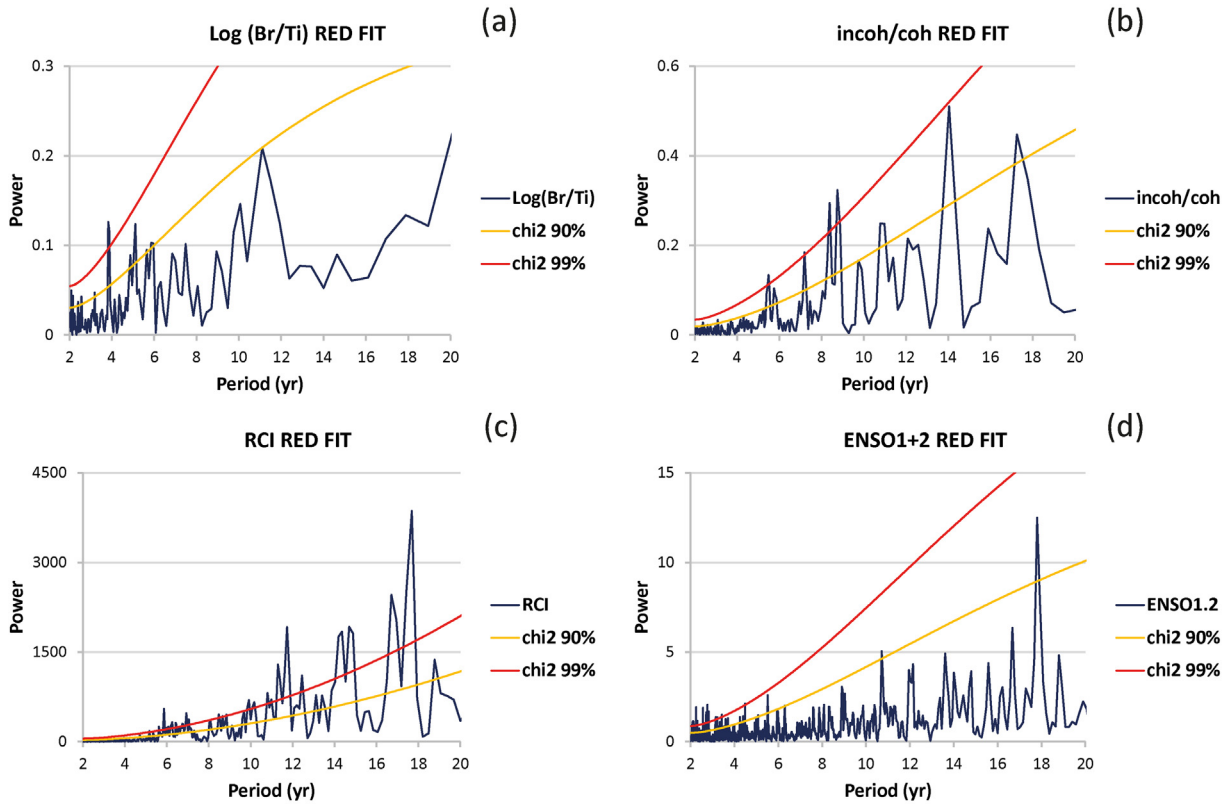

Fig. 8. RED FIT analyses for Log (Br/Ti), Inco/coh ratio, RCI and ENSO 1+2 observed in sediment core Pal IV. Spectral peaks around the 2–3 and 5–6 yr period are clearly present in both the ENSO1+2 index and the incoh./coh. ratios and RCI values in core Pal IV. Br/Ti ratios show a more pronounced 4 yr periodicity. (For interpretation of the references to colour in this figure legend, the reader is referred to the Web version of this article.)

alluvial fan which likely influenced the frequency and thickness of the fine clastic sediments in both of the depocenters of the lake. In this lower part of the catchment, recent debris flow deposits have led to avulsions of the main fluvial channels redirecting the discharge between the two sub basins. This includes the newly formed channel that recently shifted the fluvial discharge predominantly towards L. Pallcacocha's northern basin. Given the nature of avulsion on such alluvial fans, it is likely that such shifts have regularly occurred since the formation of the alluvial fan (de Haas et al, 2016, 2018a, 2018b).

4.2. The flood layer record

Our new flood layer record from the southern basin of L. Pallcacocha shows that previous sediment records (Moy et al., 2002; Rodbell et al., 1999; Schneider et al., 2018) can be reproduced from a different coring site in the same southern lake basin. This indicates that the observed flood layer record is a result of catchment processes and not in-situ lacustrine processes. Laminae are absent in the top sediments of the core from the southern basin of L. Pallcacocha, a feature that was also observed in previous sediment records from the same lake (Rodbell et al., 1999; Schneider et al., 2018). Although the homogenous top sediments were initially attributed to disturbance of the top sediment during coring (Rodbell et al., 1999), our data show that the top contains more silt and different elemental composition in both basins. This indicates that the homogenous top is a true feature in the sediments, reproduced in multiple sediment cores from the same lake (Moy et al., 2002; Rodbell et al., 1999; Schneider et al., 2018).

The absence of laminae in the top sediments of the southern basin is the result of 1) a large deposition of erodable material near the lake margin, likely as a result from a large debris flow, and 2) the abovementioned northward shift in the location of the main inflow stream. This is evidenced by an increased silt deposition in the top sediment of both basin and deposition of distinct laminae in the northern basin since ~1999 CE. Thus, spatio-temporal shifts of the fluvial channels between the northern and southern basin can affect the recording of intense rainfall events in the lithostratigraphy of L. Pallcacocha. Such fluvial shifts might have affected the lithostratigraphy in the past as well, but the Holocene infill of the northern basin shows close correspondence to the lithostratigraphy of the sediment in the southern basin, suggesting that such shifts were not critical (Appendix A). Over longer timescales (i.e. Holocene) the progradation of the alluvial fan may result in a general increase in flood layer frequency because sediment-laden discharges can reach further into the two depocenters, as suggested for the general increasing trend in flood layer frequency in lakes from the north-eastern USA (Noren et al., 2002).

Detailed chronology and frequency analyses on Br/Ti ratios, incoh./coh. ratios, and RCI values in core Pal IV from the southern basin indicates that the clastic layers in L. Pallcacocha fall into the typical ENSO 1+2 frequency band of 3, 5 and 7 years (Fig. 8). Bromine has been reported to reflect the organic content in sediments, not only from marine origin (Ziegler et al., 2008) but also terrestrial origin (Goldberg et al., 2021). As such, the log-ratio of Br/Ti in the laguna Pallcacocha records represents the deposition of organic matter versus clastic sediment input. This use of Br as an organic matter proxy is verified using the incoh/coh ratio, as incoherent radiation increases with the abundance of elements with a low atomic mass, thus often reflecting organic matter variability (e.g., Guyard et al., 2007). Indeed, the Br/Ti ratio incoh/coh ratio show similar variability, and the variability observed in these

ratios seem to also fluctuate synchronous to sediment redness, hence lithology (Rodbell et al., 1999; Moy et al., 2002) in both basins. Red color intensity was adopted by Moy et al. (2002) as the best metric of clastic events in the Pallcacocha cores. This was a change from the use of grayscale as adopted by Rodbell et al. (1999) because the RGB scale in general, and red color intensity in particular, show the greatest amplitude of change between organic and inorganic (clastic) laminae. The RCI reveals that the 1997/98 strong El Niño event is not recorded as a clastic layer in the sediments from the southern basin. The 1997/1998 El Niño activated the sediment cascade in the catchment and produced a clear clastic layer in the northern basin of the lake, instead of the usual southern basin.

Characteristic of the ENSO1+2 spectrum is the weak 5 yr component, relative to the central Pacific ENSO 3.4 index where this is a prominent periodicity. Spectral peaks around the 2–3 and 5–6 yr period are clearly present in both the ENSO1+2 index and the Br/Ti ratio, while the latter has a more pronounced 4 yr periodicity possibly due to a smoothing effect in the sediment record. The longer 5–6, 7 and ~11 yr periodicities present in the RCI and incoh/coh data are more prominent than in the ENSO1+2 index and Br/Ti. Decadal periodicities are typically recorded in other ENSO teleconnected sites sensitive to precipitation (e.g. Donders et al., 2013) and potentially linked to interaction with the solar cycle (Emile-Geay et al., 2007).

Thickness of the laminae appears to be unrelated to the strength of El Niño events. Presumably, some moderate or even weak El Niño's still had a disproportionally large impact on sediment input into the lake. This might be the effect of abundant fine-grained material left in the debris flow channels or along the margin of the lake basin prior to rainfall events, or alternatively, changes in channel pattern on the alluvial fan where a configuration with fewer but larger channels favours clastic sediments input to the lake.

5. Conclusions

Our results demonstrate the mechanisms behind the original interpretation of the flood layer record from L. Pallcacocha (Moy et al., 2002; Rodbell et al., 1999). Intense rainfall events that are often associated with coastal El Niño and Eastern Pacific ENSO events initiate debris flows in the catchment. The sediments of these debris flows deposits are transported through fluvial channels on the alluvial fan into the two sub basins of the lake, either directly or indirectly by later runoff events, producing the typical flood layer record. Lateral shifts of feeding channels within the depositional basin have led to a discrepancy in lithostratigraphy between sediment cores from the northern and southern. This can bias the reconstruction of ENSO signals from the lake's sediments. A multi-core and multi-proxy analysis are therefore essential for the interpretation of paleo-ENSO variability reconstructed from lake sediments. Detailed ^{210}Pb ages of the sediments and geochemical frequency analyses reveal that 1) the clastic layers fall into the typical ENSO band and 2) their temporal occurrence agrees within 1–2 years of instrumental El Niño records confirming the original interpretation of the flood layer record.

Declaration of competing interest

The authors declare that they have no known competing financial interests or personal relationships that could have appeared to influence the work reported in this paper.

Acknowledgements

We are grateful to Ben Heggelman, Alice Dijkema and Jos Stekelenburg from the Meander Medisch Centrum Amersfoort for their help and assistance with the CT scans. Our thanks also goes to the Ministry of Environment of Ecuador (MAE) for providing research and fieldwork permissions (permit number 009_SGA_2015_PNC_BD_VA_Donders) and the personnel from the Cajas National Park and ETAPA-EP for permitting access to the park. This research was funded by the Earth and Life Science council (ALW) of the Netherlands Organisation of Scientific Research (NWO; grant number 824.14.018).

Appendix A. Supplementary data

Supplementary data to this article can be found online at https://doi.org/10.1016/j.quascirev.2021.106900.

Credit author statement

Kimberley Hagemans: Conceptualization, Methodology, Formal analysis, Investigation, Visualization, Project administration, Writing – original draft. Kees C.A.M. Nooren: Conceptualization, Methodology, Formal analysis, Investigation, Resources, Visualization, Writing – original draft. Tjalling de Haas: Conceptualization, Methodology, Formal analysis, Visualization, Writing – review & editing. Mario Córdova: Conceptualization, Methodology, Formal analysis, Investigation, Resources, Visualization, Writing – original draft. Rick Hennekam: Methodology, Formal analysis, Investigation, Resources, Writing – review & editing. Martin C.A. Stekelenburg: Conceptualization, Methodology, Formal analysis, Investigation, Visualization, Writing – review & editing. Donald T. Rodbell: Conceptualization, Resources, Validation, Writing – review & editing. Hans Middelkoop: Conceptualization, Supervision, Writing – review & editing. Timme H. Donders: Conceptualization, Methodology, Investigation, Supervision, Funding acquisition, Project administration, Writing – review & editing.

References

Bertrand, M., Liébault, F., Piégay, H., 2013. Debris-flow susceptibility of upland catchments. Nat. Hazards 67, 497–511. https://doi.org/10.1007/s11069-013-0575-4.

Bovis, M.J., Jakob, M., 1999. The role of debris supply conditions in predicting debris flow activity. Earth Surf. Process. Landforms 24, 1039–1054. https://doi.org/10.1002/(SICI)1096-9837(199910)24:11<1039::AID-ESP29>3.0.CO;2-U.

Bussmann, F., Anselmetti, F.S., 2010. Rossberg landslide history and flood chronology as recorded in Lake Lauerz sediments (Central Switzerland). Swiss J. Geosci. 103, 43–59. https://doi.org/10.1007/s00015-010-0001-9.

Carrillo-Rojas, G., Silva, B., Córdova, M., Célleri, R., Bendix, J., 2016. Dynamic mapping of evapotranspiration using an energy balance-based model over an Andean páramo catchment of southern Ecuador. Rem. Sens. 8 https://doi.org/10.3390/rs8020160.

Colombaroli, D., Gavin, D.G., Morey, A.E., Thorndycraft, V.R., 2018. High resolution lake sediment record reveals self-organized criticality in erosion processes regulated by internal feedbacks. Earth Surf. Process. Landforms 43, 2181–2192. https://doi.org/10.1002/esp.4383.

Corbett, L.B., Munroe, J.S., 2010. Investigating the influence of hydrogeomorphic setting on the response of lake sedimentation to climatic changes in the Uinta Mountains, Utah, USA. J. Paleolimnol. 44, 311–325. https://doi.org/10.1007/s10933-009-9405-9.

de Haas, T., Densmore, A.L., Stoffel, M., Suwa, H., Imaizumi, F., Ballesteros-Cánovas, J.A., Wasklewicz, T., 2018a. Avulsions and the spatio-temporal evolution of debris-flow fans. Earth Sci. Rev. 177, 53–75. https://doi.org/10.1016/j.earscirev.2017.11.007.

de Haas, T., Kruijt, A., Densmore, A.L., 2018b. Effects of debris-flow magnitude–frequency distribution on avulsions and fan development. Earth Surf. Process. Landforms 43, 2779–2793. https://doi.org/10.1002/esp.4432.

de Haas, T., Van Den Berg, W., Braat, L., Kleinhans, M.G., 2016. Autogenic avulsion, channelization and backfilling dynamics of debris-flow fans. Sedimentology 63, 1596–1619. https://doi.org/10.1111/sed.12275" 10.1111/sed.12275.

Donders, T.H., Punyasena, S.W., De Boer, H.J., Wagner-Cremer, F., 2013. ENSO

signature in botanical proxy time series extends terrestrial El Niño record into the (sub)tropics. Geophys. Res. Lett. 40, 5776–5781.
Emile-Geay, J., Cane, M., Seager, R., Kaplan, A., Almasi, P., 2007. El Niño as a mediator of the solar influence on climate. Paleoceanography 22 (3), 1–16. https://doi.org/10.1029/2006PA001304.
Fryirs, K.A., Brierley, G.J., Preston, N.J., Kasai, M., 2007. Buffers, barriers and blankets: the (dis)connectivity of catchment-scale sediment cascades. Catena 70, 49–67. https://doi.org/10.1016/j.catena.2006.07.007.
Glur, L., Wirth, S.B., Büntgen, U., Gilli, A., Haug, G.H., Schär, C., Beer, J., Anselmetti, F.S., 2013. Frequent floods in the European Alps coincide with cooler periods of the past 2500 years. Sci. Rep. 3, 1–5. https://doi.org/10.1038/srep02770" 10.1038/srep02770.
Goldberg, T., Hennekam, R., Wasch, L., Reichart, G.-J., Rach, O., Stammeier, J.A., Griffioen, J., 2021. Suitability of calibrated X-ray fluorescence core scanning for environmental geochemical characterisation of heterogeneous sediment cores. Appl. Geochem. 125, 1–13. https://doi.org/10.1016/j.apgeochem.2020.104824.
Guyard, H., Chapron, E., St-One, G., Anselmetti, F.S., Arnaud, F., Magand, O., Francus, P., Mélières, M.A., 2007. High-altitude varve records of abrupt environmental changes and mining activity over the last 4000 years in the Western French Alps (Lake Bramant, Grandes Rousses Massif). Quat. Sci. Rev. 26, 2644–2660. https://doi.org/10.1016/j.quascirev.2007.07.007.
Guzzetti, F., Peruccacci, S., Rossi, M., Stark, C.P., 2008. The rainfall intensity-duration control of shallow landslides and debris flows: an update. Landslides 5, 3–17. https://doi.org/10.1007/s10346-007-0112-1.
Hagemans, K., Tóth, C., Ormaza, M., Gosling, W.D., Urrego, D.H., 2019. Modern Pollen-Vegetation Relationships along a Steep Temperature Gradient in the Tropical Andes of Ecuador. https://doi.org/10.1017/qua.2019.4.
Hammer, Ø., Harper, D.A.T.a.T., Ryan, P.D., 2001. PAST: paleontological statistics software package for education and data analysis. Palaeontol. Electron. 4 (1), 1–9. https://doi.org/10.1016/j.bcp.2008.05.025.
Heckmann, T., Cavalli, M., Cerdan, O., Foerster, S., Javaux, M., Lode, E., Smetanová, A., Vericat, D., Brardinoni, F., 2018. Indices of sediment connectivity: opportunities, challenges and limitations. Earth Sci. Rev. 187, 77–108. https://doi.org/10.1016/j.earscirev.2018.08.004.
Heiri, O., Lotter, A.F., Lemcke, G., 2001. Loss on ignition as a method for estimating organic and carbonate content in sediments: reproducibility and comparability of results. J. Paleolimnol. 25, 101–110.
Kiefer, J., Karamperidou, C., 2019. High-resolution modeling of ENSO-induced precipitation in the tropical Andes: implications for proxy interpretation. Paleoceanogr. Paleoclimatol. 34, 217–236. https://doi.org/10.1029/2018PA003423.
Lamoureux, S., 2002. Temporal patterns of suspended sediment yield following moderate to extreme hydrological events recorded in varved lacustrine sediments. Earth Surf. Process. Landforms 27, 1107–1124. https://doi.org/10.1002/esp.399.
Minderhoud, P.S.J., Cohen, K.M., Toonen, W.H.J., Erkens, G., Hoek, W.Z., 2016. Improving age-depth models of fluvio-lacustrine deposits using sedimentary proxies for accumulation rates. Quat. Geochronol. 33, 35–45. https://doi.org/10.1016/j.quageo.2016.01.001.
Ministerio del Ambiente del Ecuador, 2018. Actualización del plan de manejo del Parque Nactional Cajas.
Moy, C.M., Seltzer, G.O., Rodbell, D.T., Anderson, D.M., 2002. Variability of El Niño/southern oscillation activity at millennial timescales during the Holocene epoch. Nature 420, 162–165. https://doi.org/10.1038/nature01194.
NOAA, 2020. Physical Sciences Laboratory: El Niño-Southern Oscillation. https://psl.noaa.gov/enso/.
Noren, A.J., Bierman, P.R., Steig, E.J., Lini, A., Southon, J., 2002. Millennial-scale storminess variability in the northeastern United States during the Holocene epoch. Nature 419, 821–824. https://doi.org/10.1038/nature01132.
Padrón, R.S., Wilcox, B.P., Crespo, P., Célleri, R., 2015. Rainfall in the Andean páramo: new insights from high-resolution monitoring in southern Ecuador. J. Hydrometeorol. 16, 985–996. https://doi.org/10.1175/JHM-D-14-0135.1.
Rodbell, D.T., Seltzer, G.O., Anderson, D.M., Abbott, M.B., Enfield, D.B., Newman, J.H., 1999. An ~15,000-year record of El Niño-driven alluviation in southwestern Ecuador. Science 283, 516–520. https://doi.org/10.1126/science.283.5401.516.
Rubensdotter, L., Rosqvist, G., 2009. Influence of geomorphological setting, fluvial-, glaciofluvial- and mass-movement processes on sedimentation in alpine lakes. Holocene 19, 665–678. https://doi.org/10.1177/0959683609104042.
Sanchez-Cabeza, J.A., Ruiz-Fernández, A.C., 2012. 210Pb sediment radiochronology: an integrated formulation and classification of dating models. Geochem. Cosmochim. Acta 82, 183–200. https://doi.org/10.1016/j.gca.2010.12.024.
Schneider, T., Hampel, H., Mosquera, P.V., Tylmann, W., Grosjean, M., 2018. Paleo-ENSO revisited: Ecuadorian Lake Pallcacocha does not reveal a conclusive El Niño signal. Global Planet. Change 168, 54–66. https://doi.org/10.1016/j.gloplacha.2018.06.004.
Schulz, M., Mudelsee, M., 2002. REDFIT: estimating red-noise spectra directly from unevenly spaced paleoclimatic time series. Comput. Geosci. 28, 421–426. https://doi.org/10.1016/S0098-3004(01)00044-9.
Swierczynski, T., Lauterbach, S., Dulski, P., Delgado, J., Merz, B., Brauer, A., 2013. Mid- to late Holocene flood frequency changes in the northeastern Alps as recorded in varved sediments of Lake Mondsee (Upper Austria). Quat. Sci. Rev. 80, 78–90. https://doi.org/10.1016/j.quascirev.2013.08.018.
Weltje, G., Tjallingii, R., 2008. Calibration of XRF core scanners for quantitative-geochemical logging of sediment cores: theory and application. Earth Planet Sci. Lett. 274, 423–438.
Wilford, D.J., Sakals, M.E., Innes, J.L., Sidle, R.C., Bergerud, W.A., 2004. Recognition of debris flow, debris flood and flood hazard through watershed morphometrics. Landslides 1, 61–66. https://doi.org/10.1007/s10346-003-0002-0.
Ziegler, M., Jilbert, T., De Lange, G.J., Lourens, L.J., Reichart, G.-J., 2008. Bromine counts from XRF scanning as an estimate of the marine organic carbon content of sediment cores. G-cubed 9, Q05009.